Journal of Molecular Graphics and Modelling 59 (2015) 92–99

Contents lists available at ScienceDirect

Journal of Molecular Graphics and Modelling

journal homepage: www.elsevier.com/locate/JMGM

Evolution of structure, stability, and nonlinear optical properties of the heterodinuclear $CNLi_n$ (n = 1–10) clusters

Dan Hou, Di Wu, Wei-Ming Sun, Ying Li*, Zhi-Ru Li

Institute of Theoretical Chemistry, State Key Laboratory of Theoretical and Computational Chemistry, Jilin University, Liutiao Road No. 2, Changchun 130023, People's Republic of China

ARTICLE INFO

Article history:
Accepted 3 April 2015
Available online 13 April 2015

Keywords:
Nonlinear optical properties
Clusters
Superalkali
Hyperlithiated
CNLi

ABSTRACT

The lowest-energy structures and stabilities of the heterodinuclear clusters, $CNLi_n$ (n = 1–10) and relevant $CNLi_n^+$ (n = 1–10) cations, are studied using the density functional theory with the 6-311 + G(3df) basis set. The $CNLi_6$ and $CNLi_5^+$ clusters are the first three-dimensional ones in the $CNLi_n^{0/+}$ series, respectively, and the CN group always caps the $Li_n^{0/+}$ moiety in the $CNLi_n^{0/+}$ (n = 1–9) configurations. The C—N triple bond is found to be completely cleaved in the $CNLi_{10}^{0/+}$ clusters where the C and N atoms are bridged by two Li atoms. The $CNLi_n$ (n = 2–10) clusters are hyperlithiated molecules with delocalized valence electrons and consequently possess low VIP values of 3.780–5.674 eV. Especially, the $CNLi_8$ and $CNLi_{10}$ molecules exhibit lower VIPs than that of Cs atom and can be regarded as heterobinuclear superalkali species. Furthermore, these two superalkali clusters show extraordinarily large first hyperpolarizabilities of 19,423 and 42,658 au, respectively. For the $CNLi_n^+$ cationic species, the evolution of the energetic and electronic properties with the cluster size shows a special stability for $CNLi_2^+$.

1. Introduction

In the last several decades, a great number of theoretical and experimental investigations have been extensively carried out to understand the physical and chemical properties of clusters including structural and electronic properties, the nature of bonding, thermodynamic stability, *etc.* [1–8]. Experiments alone cannot provide the complete information of the clusters and only by combing them with theoretical investigations can a comprehensive description of the geometric arrangement and the corresponding properties of clusters be achieved. On the other hand, experimental data are necessary for developing a realistic theoretical model for the cluster structure [9,10]. Recently, the rapid progress in computer technology with adjacent advancements of the quantum chemical theory has provided an opportunity to explore new, unknown molecules or clusters before experimentalists can observe or synthesize them [11].

Atomic clusters can exhibit many interesting properties that are neither atom like nor extended solidlike, and show remarkable size-dependent variations. More interestingly, the properties of clusters can usually be changed by doping the clusters with other species. Hence, the pure and doped clusters have attracted numerous interested in the research field of materials as a prototype for understanding the cluster-assembled nanomaterials. Among the studied clusters, the doped lithium clusters have received considerable attention because of the well-known ability of lithium to form heterogeneous clusters with various elements. In 1978, Wu and co-workers [12] first observed Li_3O in experiment as a stable molecule in gas phase. Later, the existence of Li_4O and Li_5O was also confirmed [13]. The CLi_6 cluster was predicted and verified experimentally to be stable with respect to dissociating into the CLi_4 and Li_2 molecules [14]. These molecules with unusual stoichiometry possess valence electrons violating the octet rule, and can be regarded as hypervalent molecules. They have been named as hyperlithiated molecules after Schleyer's review [15]. Up to now, a large number of mononuclear hyperlithiated clusters of the MLi_n type have been investigated by theoretical approaches and experimental techniques, such as BLi_n [16–20], FLi_n [21,22] $BeLi_n$ and $MgLi_n$ [23–25], $AlLi_n$ [26], and $SnLi_n$ [27–29], *etc.* Usually, the hyperlithiated molecules can exhibit very low ionization potentials (IPs) because they contain delocalized excess valence electrons. For instance, the Li_3O molecule has a very low IP of 3.54 eV and can be regarded as a superalkali cluster [30].

As the first experimentally characterized binuclear hyperlithiated molecule, Li_2CN is of great interest. The Li_2CN molecule has two isomers with linear and bridged structures, respectively, and its favored structure is best described as a "salt" composed of Li_2^+ cation and CN^- anion [31]. More recently, Xu and co-workers [32]

* Corresponding author. Tel.: +86 043181707218.
E-mail address: liyingedu@jlu.edu.cn (Y. Li).

http://dx.doi.org/10.1016/j.jmgm.2015.04.004
1093-3263/

have found that the linear Li_2CN possesses a remarkably large hyperpolarizability (β_0) value of 30,1096 au and thereby can be regarded as a kind of potential nonlinear optical (NLO) molecule. Such interesting features of $CNLi_2$ inspired us to carry out a research on the larger $CNLi_n$ clusters. Recently, Roy and co-workers [33] have inserted N_2 molecule into small lithium clusters and demonstrated that at least eight lithium atoms could completely cleave the triple bonded nitrogen molecule. In our previous work, we have systemically explored the heterodinuclear system, *i.e*, $COLi_n$ (n = 2, 4, 6, 8) and $COLi_n^+$ (n = 5, 7) [34], and found that at least Li_6 or Li_7^+ cluster is needed to completely cleave the triple bond of CO. So, some interesting questions emerge: Can the triple bond of CN be reduced by small Li_n clusters likewise? How many Li atoms should be needed to cleave the CN triple bond completely? Do the IP values of $CNLi_n$ decrease with increasing number of lithium atoms? Moreover, how do the energy properties, NLO responses, binding nature, *etc.* of $CNLi_n$ evolve with the increasing cluster size?

In order to answer the above questions, the heterodinuclear clusters $CNLi_n$ (n = 1–10) and their corresponding cations have been systemically studied in the present work. First, the lowest-energy structures of $CNLi_n$ and $CNLi_n^+$ clusters were identified and compared with each other. Then, the evolution of geometrical structure, bonding nature as well as electronic and energetic properties of these species with the cluster size was investigated in detail. Results show that the $CNLi_n$ clusters exhibit superalkali nature on $CNLi_8$ and $CNLi_{10}$, which is verified by their low vertical ionization potential of 3.780 and 3.832 eV, respectively. Additionally, we also predict extraordinarily large nonlinear optical (NLO) responses of the $CNLi_4$, $CNLi_8$, and $CNLi_{10}$ clusters.

2. Computational details

We performed the search for the global minima of the $CNLi_n$ (n = 1–10) clusters on their potential energy surfaces by using the stochastic method [35–37]. This method generates structures randomly and makes the exploration of unknown isomers more thoroughly. All the atoms were initially placed at a common point in geometrical space and then kicked in random directions within a spherical shell. The setting radius of the sphere ranges from 3 Å to 10 Å in this work. Several hundred starting geometries were obtained at the B3LYP/3-21G level until no new structures appeared. Then, these structures were reoptimized with the larger 6-311 + G(3df) basis set, followed by vibrational frequency calculations. A number of isomers of the $CNLi_n$ clusters are shown in Figs. S1–S8, respectively, in the Supporting information. In addition, the single point calculations were carried out at the CCSD(T)/6-311 + G(d) level for the first five low-lying isomers of each $CNLi_n$ cluster to ensure that the global minimum was found. Then, the minimum structures of the $CNLi_n^+$ cations were obtained at the B3LYP/6-311 + G(3df) level by optimizing their corresponding $CNLi_n$ configurations upon losing an electron.

The natural bond orbital (NBO) charges [38,39] of the lowest-energy $CNLi_n$ were calculated at the B3LYP/6-311 + G(3df) level. All the single-point energy calculations of minimum structures were carried out at the CCSD(T)/6-311 + G(3df) level. Based on these single-point energies, the vertical electron affinities (VEA), vertical ionization potentials (VIP), adiabatic ionization potentials (AIP) of the $CNLi_n$ clusters, and the binding energies per atom (E_b), the second difference in energies (Δ^2E), and dissociation energies (ΔE) of the $CNLi_n$/$CNLi_n^+$ clusters were calculated in the present work, where

$$E_b(CNLi_n) = \frac{[E(C) + E(N) + nE(Li) - E(CNLi_n)]}{(n+2)}$$

$$E_b\left(CNLi_n^+\right) = \frac{\left[E(C) + E(N) + (n-1)E(Li) + E\left(Li^+\right) - E\left(CNLi_n^+\right)\right]}{(n+2)}$$

$$\Delta^2 E\left(CNLi_n^{+/0}\right) = E\left(CNLi_{n+1}^{+/0}\right) + E\left(CNLi_{n-1}^{+/0}\right) - 2E\left(CNLi_n^{+/0}\right)$$

$$\Delta E\left(CNLi_n^{+/0}\right) = E(Li) + E\left(CNLi_{n-1}^{+/0}\right) - E\left(CNLi_n^{+/0}\right)$$

The nonlinear optical (NLO) properties of the $CNLi_n$ clusters were calculated using the BhandHLYP method [40] in conjunction with the 6-311 + G(3df) basis set. The mean polarizability (α_0), and the mean first hyperpolarizability (β_0) are defined as

$$\alpha_0 = \frac{\left(\alpha_{xx} + \alpha_{yy} + \alpha_{zz}\right)}{3}$$

$$\beta_0 = \left(\beta_x^2 + \beta_y^2 + \beta_z^2\right)^{1/2}$$

$$\text{where} \quad \beta_i = \frac{3}{5}\left(\beta_{iii} + \beta_{ijj} + \beta_{ikk}\right), i, j, k = x, y, z$$

All the calculations were performed by using the GAUSSIAN 03 [41] and GAUSSIAN 09 [42] programs. The dimensional plots of molecular configurations and orbitals were generated with the GaussView [43] program (Gaussian, Inc., Pittsburgh, PA).

3. Results and discussion

3.1. Geometrical characteristics

The lowest-energy structures of $CNLi_n$ (n = 1–10) and their corresponding $CNLi_n^+$ cations are shown in Figs. 1 and 2, respectively. The highest occupied molecular orbitals (HOMOs) of the $CNLi_n$ molecules are presented in Fig. 3. The symmetry point groups, lowest vibrational frequencies, C—N distances (R_{C-N}), sum of NBO charges on C and N atoms (Q^{C+N}), and the HOMO–LUMO gaps of the $CNLi_n$ and $CNLi_n^+$ clusters are listed in Table 1.

From Fig. 1, it can be seen that the $CNLi_n$ (n = 1–5) clusters possess planar structures. Among them, the CNLi possesses a linear

Table 1
Symmetry point group, the C—N distances (R_{C-N}, in Å), the lowest vibrational frequencies (ν, in cm^{-1}) and the sum of NBO charges on C and N atoms of the most stable $CNLi_n$ (n = 1–10) and $CNLi_n^+$ (n = 1–10) clusters.

n	$CNLi_n$				$CNLi_n^+$			
	Symmetry	R_{C-N}	ν	Q^{C+N}	*Symmetry*	R_{C-N}	ν	Q^{C+N}
1	$C_{\infty v}$	1.172	118	−0.933	$C_{\infty v}$	1.150	177	0.023
2	C_s	1.168	202	−0.841	$C_{\infty v}$	1.158	128	−0.888
3	C_s	1.166	129	−0.876	$C_{\infty v}$	1.157	44	−0.859
4	C_s	1.171	88	−0.865	C_s	1.161	48	−0.826
5	C_s	1.168	79	−0.791	C_1	1.167	59	−0.814
6	C_s	1.171	54	−0.767	C_1	1.168	65	−0.780
7	C_s	1.172	115	−0.735	C_s	1.172	74	−0.770
8	C_s	1.177	76	−0.805	C_s	1.176	75	−0.836
9	C_1	1.170	39	−0.758	C_1	1.167	71	−0.754
10	C_{2v}	3.444	101	−5.288	C_{2v}	3.429	72	−5.342

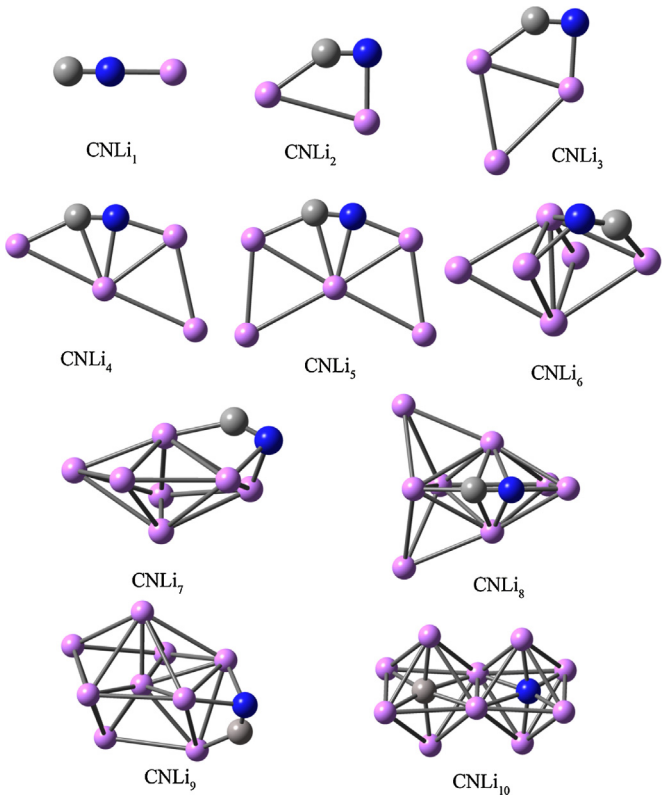

Fig. 1. The lowest-energy structures of the $CNLi_n$ (n = 1–10) clusters.

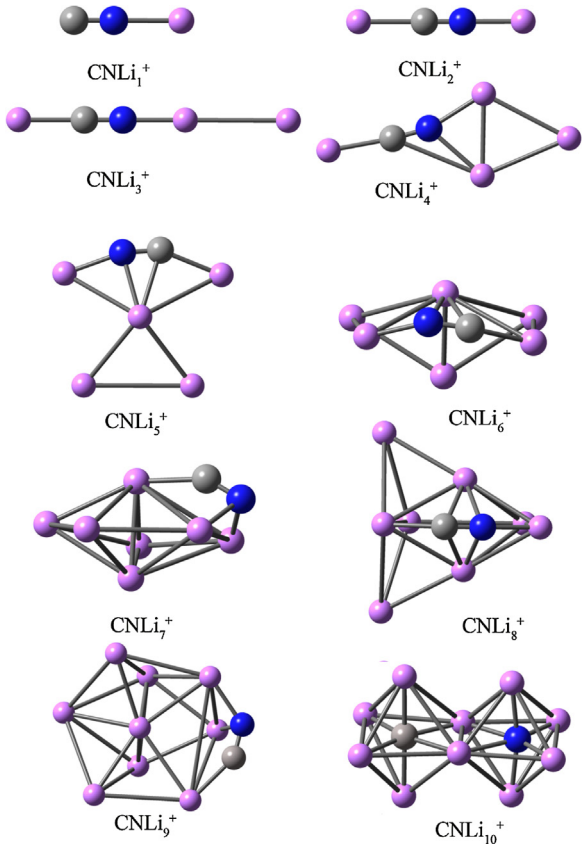

Fig. 2. The optimized minimum structures of the $CNLi_n^+$ (n = 1–10) cluster cations.

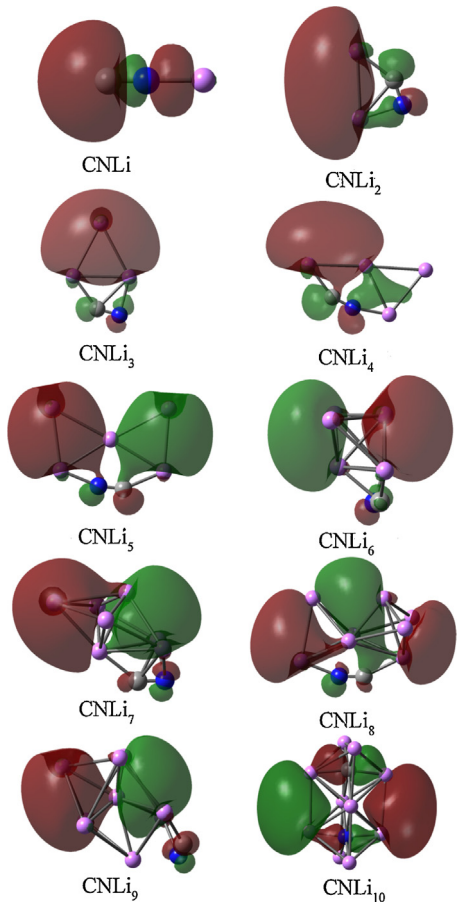

Fig. 3. The HOMO orbitals of the $CNLi_n$ clusters.

global minimum, in which the Li atom is bound to the N-side. $CNLi_2$ exhibits a trapezoid geometry in which the CN unit carries −0.841|e| NBO charge. Hence, the $CNLi_2$ cluster can be regarded as a combination of Li_2^+ and CN^-, just as reported in the literature [31]. Lately, Boldyrev and co-workers [44] performed an interesting study of ozone valence isoelectronic Li_3N_3 cluster, which possesses a similar chemical bonding pattern to that of ozone. In the present work, the valence molecular orbitals of CNLi and $CNLi_2$ and their valence isoelectronic CO and NO/CO^- molecules were compared in Figs. S9 and S10 (Supporting information), respectively. From Fig. S9, the molecular orbitals of CNLi show great resemblances to those of CO, suggesting their electronic structural similarities. This is also the case for the $CNLi_2$ molecule which has molecular orbitals much like those of its valence isoelectronic counterparts NO and CO^- (see Fig. S10). The $CNLi_3$ cluster can be generated by assembling Li_3^+ cluster with CN^-. Such a description is supported by the NBO analysis, that is, the charge on the Li_3^+ unit is 0.876|e| in the $CNLi_3$ cluster. Moreover, $CNLi_3$ can also be viewed as adding a Li atom to the Li—Li side of the $CNLi_2$ structure. It has been reported that the lowest-energy structure of Li_4 is rhombic (D_{2h}), and the most stable structures of Li_5 is a "W-shaped planar" geometry with C_{2v} symmetry [45]. In this system, the $CNLi_4$ and $CNLi_5$ can be regarded as being generated by inserting a CN unit into a Li—Li bond of the global minimum structures of Li_4 and Li_5, respectively. From NBO analysis, the $CNLi_4$ molecule is composed of Li_2^+, Li_2 and CN^- particles. The $CNLi_5$ cluster can also be taken as adding a Li atom to the $CNLi_4$ structure. To examine whether the $CNLi_5$ cluster has a more stable three-dimensional structure, the CN ligand was manually added to the optimized Li_5 and Li_5^+ structures at various positions. We optimized all the resulting structures and found that the planar

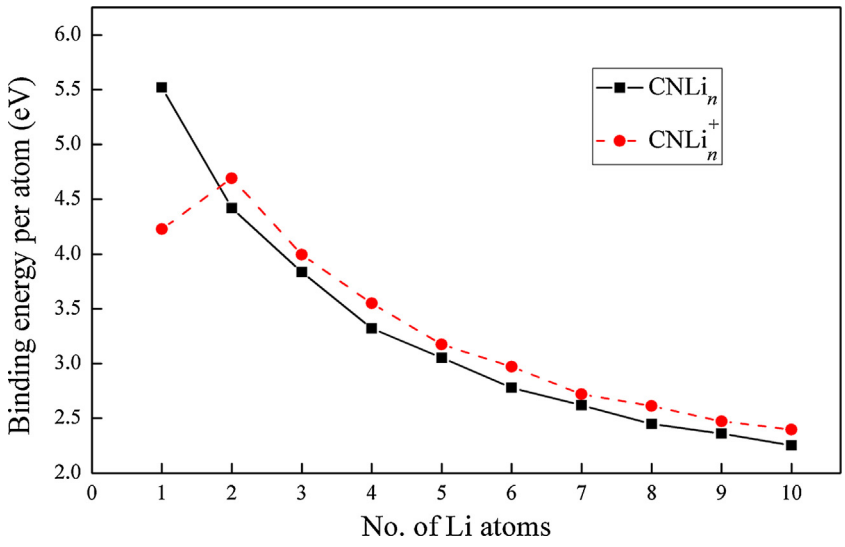

Fig. 4. The binding energies per atom (eV/atom) for the $CNLi_n$ and $CNLi_n^+$ clusters with $1 \le n \le 10$, shown as a function of the number of Li atoms.

structure is the lowest-energy one whereas the three-dimensional structures are low-lying isomers.

From $n = 6$ onwards, the $CNLi_n$ clusters began to favor three-dimensional structures. The global minima of $CNLi_6$ and $CNLi_7$ can be viewed as a CN unit face-capping the tetragonal bipyramidal Li_6 and pentagonal bipyramidal Li_7 clusters, respectively. The lowest-energy structure of $CNLi_8$ possesses C_s symmetry and could be obtained by capping two faces of $CNLi_6$ with two Li atoms. The CN unit is located in the symmetry plane of $CNLi_7$ and $CNLi_8$. The global minimum structure of $CNLi_9$ is of C_1 symmetry and features a face-capping CN unit. It is clearly seen from Fig. 1 that the CN ligand always occupies a peripheral position of the Li_n ($n < 10$) moiety. From Table 1, the CN bond lengths of $CNLi_n$ ($n = 1$–9) ranging from 1.166 Å to 1.177 Å are only 1.1–2.1% longer than that of isolated CN^- anion (1.153 Å) [46], indicating typical C—N triple bond in the $CNLi_n$ ($n = 1$–9) clusters.

Different from the above-mentioned cases, the CN unit begins to be trapped in the Li_{10} cluster. Consequently, the $CNLi_{10}$ cluster exhibits a capsule geometry of C_{2v} symmetry. Note that the C—N triple bond is completely cleaved in this structure where the C and N atoms are bridged by two Li atoms. From Table 1, the C—N distance of $CNLi_{10}$ is 3.444 Å, which are greatly longer than that of isolated CN^-. In previous works, it has been reported that eight lithium atoms are required to completely cleave the triple bond of N_2 molecule [33] and at least six lithium atoms are needed to split the C—O triple bond [34]. However, at least ten Li atoms are required to totally cleave the CN triple bond though the bond dissociation energy of 750 kJ/mol for CN^- is much lower than those of N_2 (944 kJ/mol) and CO (1076 kJ/mol) molecules [47]. Besides, different from the cases in N_2Li_n and $COLi_n$ where the N—N and C—O triple bonds were gradually reduced by Li_n in the process of triple bond → double bond → single bond → separation, the C—N bond in the $CNLi_n$ system is directly cleaved from triple bond.

From Table 1, the NBO charges ($-0.735|e|$ to $-0.933|e|$) on the CN moieties in the $CNLi_n$ ($n = 1$–9) clusters are close to -1, indicating that the CN^- group preserves its electronic integrity herein. On the other hand, the charge populations on the Li atoms indicate that the $CNLi_n$ ($n = 2$–9) species are hyperlithiated molecules, which can be supported by their molecular orbitals. From Fig. 3, the valence electrons of $CNLi_n$ ($n = 2$–9) delocalized over the lithium network. For the lowest-energy structure of $CNLi_{10}$, the sum of NBO charges on C and N atoms is $-5.288|e|$. Hence, the $CNLi_{10}$ cluster can also be described as a hyperlithiated molecule with excess valence electrons.

The optimized geometries of the $CNLi_n^+$ ($n = 1$–10) cations are shown in Fig. 2. Apparently, removal of an electron from $CNLi_n$ ($n = 1$–6) leads to elongated structures that helps to reduce the mutual repulsion interaction inside the cation, especially for $CNLi_2^+$, $CNLi_3^+$ and $CNLi_4^+$. The first three-dimensional (3D) structure in this series occurs at $CNLi_5^+$, and the structure of $CNLi_6^+$ can be regarded as generated by attaching a Li atom to the configuration of $CNLi_5^+$. From Fig. 2, it is found that losing an electron has little effect on the structures of $CNLi_n$ ($n = 7$, 8, 10), that is, the structures of $CNLi_n^+$ ($n = 7$, 8, 10) nearly coincide with the neutral parents, respectively. Likewise, at least a Li_{10}^+ cluster is needed to completely cleave the C—N triple bond.

3.2. Energetic properties

The relative stabilities of the $CNLi_n$ ($n = 1$–10) clusters are examined on the basis of the energetic properties, including the binding energy per atom (E_b), the dissociation energy (ΔE) and the second difference in energy ($\Delta^2 E$). These properties of $CNLi_n$ are listed in Table 2, and illustrated in Figs. 4–6, respectively. For comparison, the energetic properties of the corresponding $CNLi_n^+$ ($n = 1$–10) cations are also calculated and shown in Table S1 in the Supporting information and plotted in Figs. 4–6, respectively.

In general, the binding energy per atom of a mononuclear MLi_n system increases with the number of Li atoms [20,24,26,27]. However, the E_b values of the binuclear $CNLi_n$ and $CNLi_n^+$ series decrease as the cluster size increases (see Fig. 4). The maximum E_b values of the $CNLi_n$ and $CNLi_n^+$ clusters are 5.521 eV for CNLi and 4.692 eV for $CNLi_2^+$, respectively, indicating that these two clusters have relatively high stability. From Fig. 4, except for the unstable $CNLi^+$ cation, the E_b value of a cationic $CNLi_n^+$ is higher than that of its corresponding neutral one, which is similar to the case of pure Li_n clusters [45]. For the neutral Li_n and cationic Li_n^+ ($n = 2$–10) clusters, the binding energies obtained by experimental and computational methods are less than 1.15 eV [45]. From Fig. 4, the E_b values greatly rise when CN is doped into the Li_n clusters. The larger E_b values of $CNLi_n$ (2.254–5.521 eV) and $CNLi_n^+$ (2.398–4.692 eV, Table S1) than the corresponding Li_n and Li_n^+ host clusters indicate the relatively higher stability of the title clusters.

The dissociation energy (ΔE) represents the energy needed for dissociating one atom from the host cluster, namely, $CNLi_n \rightarrow CNLi_{n-1} + Li$ and $CNLi_n^+ \rightarrow CNLi_{n-1}^+ + Li$. Thus, the larger the ΔE value, the more stable the cluster is against the elimination of a Li atom. From Fig. 5, both ΔE curves show an odd–even

Table 2
Binding energy per atom (E_b, in eV), the dissociation energy (ΔE, in eV), the second difference in energy ($\Delta^2 E$, in eV), the HOMO–LUMO gaps (in eV), the vertical ionization potential (VIP, in eV), the adiabatic ionization potential (AIP, in eV), the vertical electron affinity (VEA, in eV), the hardness (η, in eV) of the most stable $CNLi_n$ (n = 1–10) clusters.

n	E_b	ΔE	$\Delta^2 E$	Gap	VIP	AIP	VEA	η
1	5.521	6.476		4.93	9.372	9.221	0.692	4.340
2	4.420	1.117	−0.384	2.04	5.110	4.251	0.536	2.287
3	3.837	1.501	0.756	2.42	5.674	4.545	0.004	2.835
4	3.321	0.746	−0.707	1.85	4.566	3.960	0.409	2.079
5	3.054	1.453	0.599	2.12	4.949	4.498	0.245	2.352
6	2.779	0.854	−0.495	1.50	4.151	3.800	0.661	1.745
7	2.620	1.349	0.457	1.66	4.552	4.443	0.500	2.026
8	2.448	0.892	−0.844	1.20	3.780	3.678	0.860	1.460
9	2.383	1.737	0.907	1.99	4.631	4.354	0.982	1.824
10	2.254	0.830		0.90	3.832	3.602	0.330	1.751

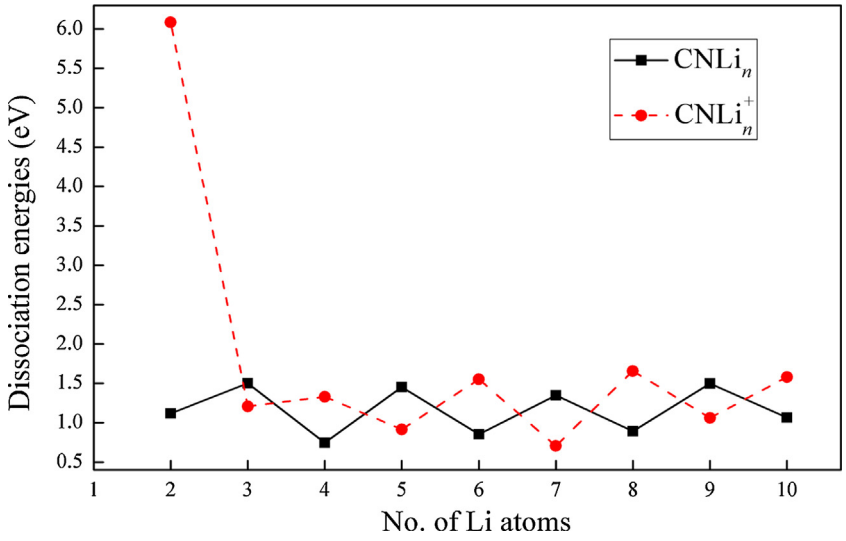

Fig. 5. The dissociation energies (ΔE, in eV) for the $CNLi_n$ and $CNLi_n^+$ clusters with $2 \le n \le 10$, shown as a function of the number of Li atoms.

pattern, demonstrating that the Li atoms are more tightly bound in closed-shell species than in open-shell ones, whether for $CNLi_n$ or $CNLi_n^+$. The conspicuous peak at $CNLi_2^+$ implies that dissociating a Li atom from $CNLi_2^+$ is an unfavorable process.

The second difference in energy ($\Delta^2 E$) of the $CNLi_n$ clusters represents a comparison between two dissociation processes, namely, $CNLi_{n+1} \rightarrow CNLi_n + Li$ and $CNLi_n \rightarrow CNLi_{n-1} + Li$. A positive $\Delta^2 E$ value indicates that the dissociation of $CNLi_{n+1}$ into $CNLi_n$ is a more favorable process than the fragmentation of $CNLi_n$ into $CNLi_{n-1}$, and the same is true for $CNLi_n^+$. Therefore, $\Delta^2 E > 0$ means that the $CNLi_n$ and $CNLi_n^+$ clusters are particularly stable. Besides, the tips of the $\Delta^2 E$ curves indicate relatively high stability of the

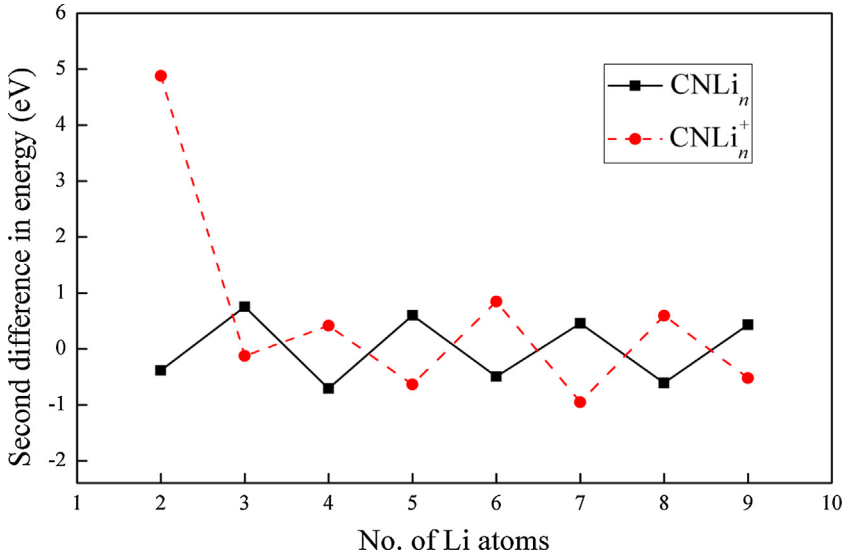

Fig. 6. The second difference in energy ($\Delta^2 E$, in eV) for the $CNLi_n$ and $CNLi_n^+$ clusters with $2 \le n \le 9$, shown as a function of the number of Li atoms.

corresponding species. From Fig. 6, both the curves of $CNLi_n$ and $CNLi_n^+$ show clear odd–even oscillations. That is to say, the species with closed electronic shell are relatively stable compared with open-shell ones. Note that the $CNLi_2^+$ cluster exhibits a significantly large Δ^2E value of 4.879 eV, indicating its special stability among all the clusters considered in this study. Positive Δ^2E values are presented for $CNLi_3$ (0.756 eV), $CNLi_5$ (0.599 eV), $CNLi_7$ (0.457 eV), $CNLi_9$ (0.907 eV), $CNLi_2^+$ (4.879 eV), $CNLi_4^+$ (0.415 eV), $CNLi_6^+$ (0.847 eV), $CNLi_8^+$ (0.596 eV), showing their relative stabilities.

3.3. Electronic properties

The electronic properties of the $CNLi_n$ clusters can be reflected by highest occupied–lowest unoccupied molecular orbital (HOMO–LUMO) energy gaps, vertical ionization potential (VIP), adiabatic ionization potential (AIP), vertical electron affinities (VEA), and global chemical hardness (η). These properties of $CNLi_n$ are shown in Table 2 and Fig. S11.

The HOMO–LUMO energy gap, as is well-known, is a useful quantity for examining the electronic stability of clusters. It is found that the systems with large HOMO–LUMO gaps are, in general, less reactive. From Table 2, the $CNLi_n$ clusters show large HOMO–LUMO energy gaps of 0.90–4.93 eV, and the stable salt molecule CNLi possesses the largest gap value among these species. As is shown in Table S1, the $CNLi_n^+$ cations show larger HOMO–LUMO gaps than their corresponding neutral parents no matter whether the cluster is closed-shell or not. Hence, the cationic species are more stable than the neutral ones. An exception here is the $CNLi^+$ cation where the CN ligand is almost neutral and in an unstable electron-deficient state. Consequently, the gap value of $CNLi^+$ is as small as 0.18 eV. In contrast, the $CNLi_2^+$ cation exhibits a quite large gap value of 8.57 eV because it does not contain any delocalized valence electron.

Ionization potential (IP) is defined as the amount of energy required to remove an electron from a molecule. Thus, a lower IP of neutral molecule means that the generation of the corresponding cation is more feasible. In our case the vertical ionization potential (VIP) is determined as the energy difference between $CNLi_n$ and its ionized cluster at the optimized geometry of $CNLi_n$, while the adiabatic ionization potential (AIP) is calculated as the energy difference between $CNLi_n$ and the corresponding cationic $CNLi_n^+$ at their respective optimized geometries. Therefore, the VIP values are always larger than the AIPs with the energy difference derived from structure relaxation, as shown in Table 2. From Table 2 and Fig. S11, the VIPs of $CNLi_n$ are quite close to the AIP values when n = 1, 7, 8 and 10 because these clusters possess similar geometrical structures to the corresponding cationic ones. In contrast, the differences between VIPs and AIPs of $CNLi_n$ (n = 2–6, 9) are considerable, especially for the $CNLi_2$ and $CNLi_3$ clusters.

As expected, the $CNLi_n$ (n = 2–10) clusters have low VIP values of 3.780–5.674 eV, which are comparable to or slightly higher than that of Li atom. This feature accords well with their hyperlithiated molecule identity. The VIPs of 3.780 and 3.832 eV for the $CNLi_8$ and $CNLi_{10}$ clusters are even lower than the IP = 3.89 eV for Cs atom, hence these two clusters can be regarded as heterobinuclear superalkali species.

The vertical electron affinities (VEA) of $CNLi_n$ are determined as VEA = E (optimized neutral) − E (anion at optimized neutral geometry). As one can notice from Table 2, all the VEA values (0.004–0.982 eV) of the $CNLi_n$ clusters are very low, indicating their stability against addition of an electron. Besides, there are clear dips at $CNLi_3$, $CNLi_5$, $CNLi_7$, and $CNLi_{10}$ in the VEA curve, suggesting that these clusters are less likely to gain an electron than the other ones. Compared with previously reported results, it is interesting to find that the VEA value of 3.285 eV for heterobinuclear $CNLi_8^+$ is just between those of homobinuclear superalkali cations $C_2Li_9^+$ (3.40 eV) [48] and $N_2Li_7^+$ (3.08 eV) [48].

With the knowledge of the ionization potential and the electron affinity, it is possible to calculate the global chemical hardness (η) [49], which can be approximated as,

$$\eta \approx \frac{1}{2}(\mathrm{VIP} - \mathrm{VEA})$$

The hardness is a useful measurement for examining the stability of clusters. Structures with large hardness values are often considered to be harder, namely, less reactive and more stable. From Table 2 and Fig. S11, it is noted that the hardness values of the $CNLi_n$ clusters tend to decrease with increasing cluster size. Meanwhile, the clear peaks at n = 3, 5, 7 and 9 imply the relative stability of the closed-shell clusters.

3.4. Nonlinear optical (NLO) properties

The NLO response of the $CNLi_n$ clusters is also investigated by evaluating their (hyper)polarizabilities. First, we performed our test calculation on the chosen open-shell $CNLi_2$ and closed-shell $CNLi_3$ by using the B3LYP, BhandHLYP, MP2 and CAM-B3LYP [50] methods in conjunction with the 6-311 + G(3df) basis set, and the results are given in Table S2 in the Supporting information. As can be seen from the table, on the whole, the BhandHLYP results agree well with the MP2 values. For example, the β_0 values of $CNLi_2$ and $CNLi_3$ at the BhandHLYP level are 9.8% and 2.0% lower than the MP2 results, respectively. Thus, the more time-saving BhandHLYP method was chosen to calculate the NLO properties of the $CNLi_n$ clusters.

The resulting static polarizabilities (α_0) and first hyperpolarizabilities (β_0) of the $CNLi_n$ clusters are listed in Table 3. Since the electrons are delocalized in the $CNLi_n$ (n = 2–10) clusters (see Fig. 3), we consider that these hyperlithiated clusters are easily polarizable and can be expected to have large polarizabilities. From Table 3, the α_0 values of $CNLi_n$ (n = 2–10) range from 149.17 to 770.47 au, which are much larger than that of 23.63 au for the CNLi molecule. Besides, it can be seen that the α_0 values increase with the increasing cluster size. To investigate the NLO properties, we focused on the first hyperpolarizabilities (β_0). From Table 3, the β_0 value of the lowest-energy structure of $CNLi_2$ is 4034 au, which is not so large as that of its low-lying linear isomer [32]. The $CNLi_4$, $CNLi_8$, and $CNLi_{10}$ clusters show remarkably large first hyperpolarizabilities of 14,238–42,658 au, while the other $CNLi_n$ clusters exhibit β_0 values in the range of 3623–4034 au. Unlike the hyperlithiated $CNLi_n$ (n = 2–10) compounds with considerable β_0 values, the β_0 value of CNLi is only 65 au. Our results also show that the β_0 values of open-shell $CNLi_n$ clusters are relatively larger compared with those of closed-shell ones.

From a physical standpoint, the first hyperpolarizability β_0 is expressed by the "sum-over-states" (SOS) expression in theory, Oudar and Chemla established a simple link between the β_0 and a low-lying charge-transfer transition by the two-level model [51,52]. For the static case (ω = 0.0), the following expression is employed to estimate β_0:

$$\beta_0 \propto \frac{\Delta\mu \times f_0}{\Delta E^3}$$

where the ΔE, f_0, and $\Delta\mu$ represent the transition energy, oscillator strength and the difference of the dipole moment between the ground state and the crucial excited state, respectively. According to the two-level model, the low transition energy is the decisive factor for a large β_0 value. From Table 3, the crucial transition energy (ΔE) values of 1.338–2.780 eV for the $CNLi_n$ (n = 2–10) clusters are pretty small compared with that of 7.230 eV for the CNLi molecule.

Table 3
The polarizabilities (α_0, in au), the first hyperpolarizabilities (β_0, in au), the crucial transition energies (ΔE, in eV) and oscillator strengths (f_0) of the most stable $CNLi_n$ (n = 1–10) clusters.

n	α_{xx}	α_{yy}	α_{zz}	α_0	β_0	f_0	ΔE
1	20.27	20.27	30.35	23.63	65	0.1174	7.230
2	197.75	119.39	130.38	149.17	4034	0.1530	1.353
3	166.79	189.38	145.95	167.37	3957	0.3365	2.269
4	455.16	260.15	240.26	318.52	14,238	0.2903	2.484
5	469.53	293.41	252.64	338.53	3632	0.3311	2.160
6	314.76	530.81	434.84	426.80	3846	0.2720	1.955
7	382.68	448.82	533.38	454.96	3623	0.6445	2.270
8	817.29	495.40	597.61	636.77	19,423	0.1991	2.056
9	499.36	524.09	520.21	514.55	3715	0.4715	2.780
10	948.08	664.96	698.38	770.47	42,658	0.2844	1.338

As a result, the hyperlithiated $CNLi_n$ clusters exhibit considerably large β_0 values.

4. Conclusions

In summary, we have theoretically investigated a new type of heterodinuclear hyperlithiated clusters $CNLi_n$ and its corresponding $CNLi_n^+$ cluster cations. The lowest-energy geometries for these CN-doped Li clusters are revealed by employing the density functional theory. It is found that removal of an electron from $CNLi_n$ (n = 1–6) leads to elongated structures, especially for $CNLi_2$, $CNLi_3$, and $CNLi_4$. In contrast, losing an electron has little effect on the latter $CNLi_n$ clusters and the structures of $CNLi_n^+$ (n = 7, 8, 10) almost coincide with the neutral parents, respectively. Different from the cases in N_2Li_n and $COLi_n$ where the N—N and C—O triple bonds were gradually reduced by Li_n, the C—N triple bond in the $CNLi_n^{0/+}$ system is directly cleaved by the $Li_{10}^{0/+}$ cluster. The $CNLi_8$ and $CNLi_{10}$ clusters featuring considerable low VIPs of 3.780 and 3.832 eV, respectively, and can be regarded as heterobinuclear superalkali species. Meanwhile, such clusters exhibit considerable NLO responses with large first hyperpolarizabilities (β_0) of 19,423 and 42,658 au, respectively.

Acknowledgements

This work was supported by the National Natural Science Foundation of China (grant nos. 21173095, 21173098, 21303066) and the National Basic Research Program of China (2013CB834801).

Appendix A. Supplementary data

Supplementary data associated with this article can be found, in the online version, at http://dx.doi.org/10.1016/j.jmgm.2015.04.004

References

[1] T. Bergmann, H. Limberger, T. Martin, Evidence of electronic shell structure in Cs–O clusters, Phys. Rev. Lett. 60 (1988) 1767.
[2] V. Bonacic-Koutecky, P. Fantucci, J. Koutecky, Quantum chemistry of small clusters of elements of groups Ia, Ib, and IIa: fundamental concepts, predictions, and interpretation of experiments, Chem. Rev. 91 (1991) 1035–1108.
[3] P. Jena, S.N. Behera, Clusters and Nanostructured Materials, Nova Science, New York, 1996.
[4] J. Niu, B. Rao, P. Jena, Atomic and electronic structures of neutral and charged boron and boron-rich clusters, J. Chem. Phys. 107 (1997) 132–140.
[5] X. Li, H. Wu, X.-B. Wang, L.-S. Wang, S–p hybridization and electron shell structures in aluminum clusters: a photoelectron spectroscopy study, Phys. Rev. Lett. 81 (1998) 1909.
[6] A.E. Kuznetsov, J.D. Corbett, L.S. Wang, A.I. Boldyrev, Aromatic mercury clusters in ancient amalgams, Angew. Chem. Int. Ed. 40 (2001) 3369–3387.
[7] R.R. Zope, S.A. Blundell, T. Baruah, D.G. Kanhere, Density functional study of structural and electronic properties of Na_nMg ($1 \le n \le 12$) clusters, J. Chem. Phys. 115 (2001) 2109.
[8] J. Xiang, S.H. Wei, X.H. Yan, J.Q. You, Y.L. Mao, A density-functional study of Al-doped Ti clusters: Ti_nAl (n = 1–13), J. Chem. Phys. 120 (2004) 4251–4257.
[9] S. Heiles, R.L. Johnston, Global optimization of clusters using electronic structure methods, Int. J. Quant. Chem. 113 (2013) 2091–2109.
[10] R.P. Hoffmann, v.R. Schleyer, H.F. Schaefer, Predicting molecules—more realism, Angew. Chem. Int. Ed. 47 (2008) 7164–7167.
[11] A.S. Ivanov, A.I. Boldyrev, Reliable predictions of unusual molecules, Phys. Chem. Chem. Phys. 14 (2012) 15943–15952.
[12] C. Wu, H. Kudo, H. Ihle, Thermochemical properties of gaseous Li_3O and Li_2O_2, J. Chem. Phys. 70 (1979) 1815–1820.
[13] C. Wu, The stability of the molecules Li_4O and Li_5O, Chem. Phys. Lett. 139 (1987) 357–359.
[14] H. Kudo, Observation of Hypervalent CLi_6 by Knudsen-Effusion Mass Spectrometry, Nature 355 (1992) 432–434 (30 January 1992).
[15] P.v.R. Schleyer, E.U. Wuerthwein, J.A. Pople, Effectively hypervalent first-row molecules. 1. Octet rule violations by OLi_3 and OLi_4, J. Am. Chem. Soc. 104 (1982) 5839–5841.
[16] Y. Li, Y.-J. Liu, D. Wu, Z.-R. Li, Evolution of the structures and stabilities of boron-doped lithium cluster cations: ab initio and DFT studies, Phys. Chem. Chem. Phys. 11 (2009) 5703–5710.
[17] K.A. Nguyen, G.N. Srinivas, T.P. Hamilton, K. Lammertsma, Stability of hyperlithiated borides, J. Phys. Chem. A 103 (1999) 710–715.
[18] K.A. Nguyen, K. Lammertsma, Structure, bonding, and stability of small boron-lithium clusters, J. Phys. Chem. A 102 (1998) 1608–1614.
[19] A. Meden, J. Mavri, M. Bele, S. Pejovnik, Dissolution of boron in lithium melt, J. Phys. Chem. 99 (1995) 4252–4260.
[20] T.B. Tai, P.V. Nhat, M.T. Nguyen, S. Li, D.A. Dixon, Electronic structure and thermochemical properties of small neutral and cationic lithium clusters and boron-doped lithium clusters: $Li_n^{0/+}$ and $Li_nB^{0/+}$ (n = 1–8), J. Phys. Chem. A 115 (2011) 7673–7686.
[21] O.M. Nešković, M.V. Veljković, S.R. Veličković, L.T. Petkovska, A.A. Perić-Grujić, Ionization energies of hypervalent Li_2F, Li_2Cl and Na_2Cl molecules obtained by surface ionization electron impact neutralization mass spectrometry, Rapid Commun. Mass. Spectrom. 17 (2003) 212–214.
[22] S.R. Veličković, V.J. Koteski, J.N. Beloševićx Čavor, V.R. Djordjević, J.M. Cvetićanin, J.B. Djustebek, et al., Experimental and theoretical investigation of new hypervalent molecules Li_nF (n = 2–4), Chem. Phys. Lett. 448 (2007) 151–155.
[23] T. Baruah, D. Kanhere, R.R. Zope, Topological study of charge densities of impurity doped small Li clusters, Phys. Rev. A: At. Mol. Opt. Phys. 63 (2001) 063202.
[24] M. Deshpande, A. Dhavale, R. Zop, S. Chacko, D. Kanhere, Ground-state geometries and stability of impurity doped clusters: Li_nBe and Li_nMg (n = 1–12), Phys. Rev. A: At. Mol. Opt. Phys. 62 (2000) 063202.
[25] R.-q. Tang, Electronic structure of small clusters of Li and a Li–Mg compound, Phys. Rev. B: Condens. Matter 43 (1991) 9255.
[26] H.-P. Cheng, R. Barnett, U. Landman, Energetics and structures of aluminum–lithium clusters, Phys. Rev. B: Condens. Matter 48 (1993) 1820.
[27] S. Shetty, S. Pal, D.G. Kanhere, A study of electronic and bonding properties of Sn doped Li_n clusters and aluminum based binary clusters through electron localization function, J. Chem. Phys. 118 (2003) 7288.
[28] K. Joshi, D. Kanhere, Finite temperature behavior of impurity doped lithium cluster, Li_6Sn, J. Chem. Phys. 119 (2003) 12301–12307.
[29] K. Joshi, D. Kanhere, Ab initio investigation of electronic structure, equilibrium geometries, and finite-temperature behavior of Sn-doped Li_n clusters, Phys. Rev. A: At. Mol. Opt. Phys. 65 (2002) 043203.
[30] G.L. Gutsev, A.I. Boldyrev, DVM Xα calculations on the electronic structure of superalkali cations, Chem. Phys. Lett. 92 (1982) 262–266.
[31] H. Kudo, M. Hashimoto, K. Yokoyama, C. Wu, A.E. Dorigo, F.M. Bickelhaupt, et al., Structure and stability of the Li_2CN molecule: an experimental and ab initio study, J. Phys. Chem. 99 (1995) 6477–6482.
[32] R.-L. Zhong, H.-L. Xu, S. Muhammad, J. Zhang, Z.-M. Su, The stability and nonlinear optical properties: encapsulation of an excess electron compound $LiCN\cdots Li$ within boron nitride nanotubes, J. Mater. Chem. 22 (2012) 2196.
[33] D. Roy, A. Navarro-Vazquez, P.v.R. Schleyer, Modeling dinitrogen activation by lithium: a mechanistic investigation of the cleavage of N_2 by stepwise insertion into small lithium clusters, J. Am. Chem. Soc. 131 (2009) 13045–13053.

[34] Y.-J. Xi, Y. Li, D. Wu, Z.-R. Li, Theoretical study of the $COLi_n$ complexes: interaction between carbon monoxide and lithium clusters of different sizes, Comput. Theor. Chem. 994 (2012) 6–13.
[35] D. Roy, C. Corminboeuf, C.S. Wannere, R.B. King, P.v.R. Schleyer, Planar tetracoordinate carbon atoms centered in bare four-membered rings of late transition metals, Inorg. Chem. 45 (2006) 8902–8906.
[36] P.P. Bera, K.W. Sattelmeyer, M. Saunders, H.F. Schaefer, P.v.R. Schleyer, Mindless chemistry, J. Phys. Chem. A 110 (2006) 4287–4290.
[37] M. Saunders, Stochastic search for isomers on a quantum mechanical surface, J. Comput. Chem. 25 (2004) 621–626.
[38] J. Carpenter, F. Weinhold, Analysis of the geometry of the hydroxymethyl radical by the different hybrids for different spins natural bond orbital procedure, J. Mol. Struct.: THEOCHEM 169 (1988) 41–62.
[39] A.E. Reed, R.B. Weinstock, F. Weinhold, Natural population analysis, J. Chem. Phys. 83 (1985) 735–746.
[40] C. Lee, W. Yang, R.G. Parr, Development of the Colle–Salvetti correlation-energy formula into a functional of the electron density, Phys. Rev. B: Condens. Matter 37 (1988) 785–789.
[41] M.J. Frisch, G.W. Trucks, H.B. Schlegel, G.E. Scuseria, M.A. Robb, J.R. Cheeseman, J.A. Montgomery Jr., T. Vreven, K.N. Kudin, J.C. Burant, J.M. Millam, S.S. Iyengar, J. Tomasi, V. Barone, B. Mennucci, M. Cossi, G. Scalmani, N. Rega, G.A. Petersson, H. Nakatsuji, M. Hada, M. Ehara, K. Toyota, R. Fukuda, J. Hasegawa, M. Ishida, T. Nakajima, Y. Honda, O. Kitao, H. Nakai, M. Klene, X. Li, J.E. Knox, H.P. Hratchian, J.B. Cross, V. Bakken, C. Adamo, J. Jaramillo, R. Gomperts, R.E. Stratmann, O. Yazyev, A.J. Austin, R. Cammi, C. Pomelli, J.W. Ochterski, P.Y. Ayala, K. Morokuma, G.A. Voth, P. Salvador, J.J. Dannenberg, V.G. Zakrzewski, S. Dapprich, A.D. Daniels, M.C. Strain, O. Farkas, D.K. Malick, A.D. Rabuck, K. Raghavachari, J.B. Foresman, J.V. Ortiz, Q. Cui, A.G. Baboul, S. Clifford, J. Cioslowski, B.B. Stefanov, G. Liu, A. Liashenko, P. Piskorz, I. Komaromi, R.L. Martin, D.J. Fox, T. Keith, M.A. Al-Laham, C.Y. Peng, A. Nanayakkara, M. Challacombe, P.M.W. Gill, B. Johnson, W. Chen, M.W. Wong, C. Gonzalez, J.A. Pople, Gaussian 03, Revision C.02, Gaussian, Inc, Wallingford, CT, 2004.
[42] M.J. Frisch, G.W., Trucks, H.B., Schlegel, G.E., Scuseria, M.A., Robb, J. R. Cheeseman, G., Scalmani, V., Barone, B., Mennucci, G.A., Petersson, H., Nakatsuji, M., Caricato, X., Li, H.P., Hratchian, A.F., Izmaylov, J., Bloino, G., Zheng, J.L., Sonnenberg, M., Hada, M., Ehara, K., Toyota, R., Fukuda, J., Hasegawa, M., Ishida, T., Nakajima, Y., Honda, O., Kitao, H., Nakai, T., Vreven, J. A. Montgomery, Jr., J. E. Peralta, F., Ogliaro, M., Bearpark, J.J., Heyd, E., Brothers, K.N., Kudin, V. N. Staroverov, R., Kobayashi, J., Normand, K., Raghavachari, A., Rendell, J.C., Burant, S.S., Iyengar, J., Tomasi, M., Cossi, N., Rega, J.M., Millam, M., Klene, J.E., Knox, J.B., Cross, V., Bakken, C., Adamo, J., Jaramillo, R., Gomperts, R.E., Stratmann, O., Yazyev, A.J., Austin, R., Cammi, C., Pomelli, J.W., Ochterski, R.L., Martin, K., Morokuma, V.G., Zakrzewski, G.A., Voth, P., Salvador, J.J., Dannenberg, S., Dapprich, A.D. Daniels, Ö. Farkas, J.B., Foresman, J.V., Ortiz, J. Cioslowski, and D.J. Fox, Gaussian, Inc., Wallingford CT, (2009) Gaussian 09, Revision A.02.
[43] R. Dennington, T. Keith, J. Millam, GaussView, Version 5, Semichem, Inc., Shawnee Mission, KS, 2009.
[44] J.K. Olson, A.S. Ivanov, A.I. Boldyrev, All-nitrogen analogue of ozone: Li_3N_3 species, Chem. Eur. J. 20 (2014) 6636–6640.
[45] N. Goel, S. Gautam, K. Dharamvir, Density functional studies of Li_n and Li_n^+ (n = 2–30) clusters: structure, binding and charge distribution, Int. J. Quantum Chem. 112 (2012) 575–586.
[46] A.E. Douglas, D. Sharma, Rotation-vibration spectra of diatomic and simple polyatomic molecules with long absorbing Paths IX. The spectra of the HCN and DCN molecules from 2.5 μ to 0.5 μ, J. Chem. Phys. 21 (1953) 448–458.
[47] Y.R. Luo, Comprehensive Handbook of Chemical Bond Energies, CRC Press, 2007.
[48] J. Tong, Y. Li, D. Wu, Z.R. Li, X.R. Huang, Ab initio investigation on a new class of binuclear superalkali cations $M_2Li_{2k+1}^+$ ($F_2Li_3^+$, $O_2Li_5^+$, $N_2Li_7^+$, and $C_2Li_9^+$), J. Phys. Chem. A 115 (2011) 2041–2046.
[49] R.G. Parr, R.G. Pearson, Absolute hardness: companion parameter to absolute electronegativity, J. Am. Chem. Soc. 105 (1983) 7512–7516.
[50] Y. Tawada, T. Tsuneda, S. Yanagisawa, T. Yanai, K. Hirao, A long-range-corrected time-dependent density functional theory, J. Chem. Phys. 120 (2004) 8425–8433.
[51] J.d. Oudar, Optical nonlinearities of conjugated molecules. Stilbene derivatives and highly polar aromatic compounds, J. Chem. Phys. 67 (1977) 446–457.
[52] J.-L. Oudar, D. Chemla, Hyperpolarizabilities of the nitroanilines and their relations to the excited state dipole moment, J. Chem. Phys. 66 (1977) 2664–2668.